Sustainable Energy & Fuels

ROYAL SOCIETY OF CHEMISTRY

PAPER

View Article Online
View Journal | View Issue

Cite this: *Sustainable Energy Fuels*, 2023, 7, 5361

On the understanding of bio-oil formation from the hydrothermal liquefaction of organosolv lignin isolated from softwood and hardwood sawdust†

Petter Paulsen Thoresen,[a] Jonas Fahrni,[b] Heiko Lange,[acd] Jasmine Hertzog,[e] Vincent Carré,[e] Ming Zhou,[f] Anna Trubetskaya,[g] Frédéric Aubriet,[e] Jonas Hedlund,[f] Tomas Gustafsson,[b] Ulrika Rova,[a] Paul Christakopoulos[a] and Leonidas Matsakas *[a]

Received 28th July 2023
Accepted 3rd October 2023

DOI: 10.1039/d3se00976a

rsc.li/sustainable-energy

Conversion of organosolv lignins isolated with and without an inorganic acid catalyst (H_2SO_4) from hard- and softwood (birch and spruce) into bio-oil through hydrothermal liquefaction has been investigated. Furthermore, fractions of the isolated bio-oils were catalytically deoxygenated to improve the bio-oil properties. As elucidated through NMR, both biomass source and extraction mode influence the bio-oil product distribution. Depending on whether the lignins carry a high content of native structures, or are depolymerized and subsequently condensed in the presence of sugar dehydration products, will dictate heavy oil (HO) and light oil (LO) distribution, and skew the HO product composition, which again will influence the requirements upon catalytical deoxygenation.

Introduction

Several issues are up for discussion when considering the persistent use and recovery of fossil fuels and petroleum. First, our economy and modern society are essentially founded on the idea that these resources are readily available.[1] The abundance of non-renewable carbon is not completely known, its accessibility uncertain, so exactly when we will experience 'peak oil' and for how long these reserves will last, is questionable.[2] The second discussion concerning the impact of fossil carbon on the climate is, to a larger extent, experiencing consensus,[3] and the possible detrimental scenarios induced by extreme weather conditions include shortages of food, fresh drinking water, and outbreaks of diseases.[4,5] Thus, even though the reserves of petroleum might, and likely will, sustain for several decades to come, the persistent usage of these will eventually be forced to a halt, and the global consequences upon on their depletion will be largely damaging for life as we know it today.

A potential shift from traditional petroleum-based chemicals toward renewable ones is receiving increasing attention because of the aforementioned concerns.[6] Especially the lignin fraction of lignocellulosic biomass is nowadays considered largely unexploited relative to its potential as the largest renewable source of aromatics.[7] However, the main issue regarding achieving proper utilization of this vastly abundant component, moving toward integrating it as an industrial, aromatic building-block and mitigate toward lower global greenhouse gas emission, is to be established.[8]

To aid in overcoming this hurdle, the present work evaluates both an effective way of extracting this underutilized polymer, and its subsequent conversion into low molecular weight components in the form of bio-oil. This final bio-oil carries the potential of replacing important chemicals for the industry. For the initial lignin extraction process, organosolv fractionation was applied. This technology has over the recent years been well explored, with several recent papers reviewing the current state, and issues to be solved.[9,10] Meanwhile, the key idea behind the process is to apply an extraction solution often consisting of water and organic solvents such as alcohols, organic acids or ketones,[11] sometimes with the addition of a catalyst,[12] which often has a profound effect on the chemistry of the obtained extract.[13] Another important factor determining the chemistry of the obtained lignin isolate, is the type of raw material (hardwood, softwood or herbaceous raw material).[14] While this extraction yields a product, which can be isolated to give lignin of high purity, the isolate will still be highly dispersed when

[a]*Biochemical Process Engineering, Division of Chemical Engineering, Department of Civil, Environmental and Natural Resources Engineering, Luleå University of Technology, 971-87, Sweden. E-mail: leonidas.matsakas@ltu.se; Tel: +46 (0) 920 493043*

[b]*RISE Processum AB, Department Biorefinery and Energy, Division of Bioeconomy and Health, Research Institute of Sweden, 981 22 Örnsköldsvik, Sweden*

[c]*Department of Earth and Environmental Sciences, University of Milano-Bicocca, Piazza della Scienza 1, 20126 Milan, Italy*

[d]*NBFC – National Biodiversity Future Center, 90133 Palermo, Italy*

[e]*Université de Lorraine, LCP-A2MC, 57000 Metz, France*

[f]*Chemical Technology, Luleå University of Technology, 971 87 Luleå, Sweden*

[g]*Department of Bioscieces, Nord University, 7713 Steinkjer, Norway*

† Electronic supplementary information (ESI) available. See DOI: https://doi.org/10.1039/d3se00976a

considering its inherent composition and chemical structures. Thus, a subsequent treatment would be necessary to retrieve aromatic monomers with direct applications in the chemical industry. Hydrothermal liquefaction (HTL) is a way to achieve this.[15] Application of this method for valorizing lignins into compounds of lower molecular weight is highly complex, both as a result of the initial lignin chemistry, but also because of the somewhat chaotic character of subcritical water where depolymerisation, decomposition, and recombination occur at the same time.[16] For these reasons, the present work sets out to provide insight into how the initial lignin chemistry affects the distribution of the obtained bio-oil phases (volatiles (V), LO, HO, char (C)) but also the release of specific components seemingly originating from certain lignin motifs, or if specific motifs favors the formation of any product phase over the other. Finally, and for bringing the generated bio-oil fractions into suitable fuel components, catalytical upgrading will be performed. A recent work summarized the current state of catalytic deoxygenation of bio-mass derived fuel-precursors,[17] and whereas the specific catalyst in combination with the precursors and its deoxygenation route varies, it essentially depends in the stability of the oxygen carrying group. This in general renders furan compounds harder to deoxygenate than phenols due to the integral role of the oxygen in the aromatic system.

Zeolites are the most prospective candidates for the upgrading of bio-oil attribute to their high hydrothermal stability, adjustable acidity, controllable pore structure, and shape selectivity. Especially, it has been noticed that ZSM-5 type zeolites have the perfect acidity and pore size for cracking and aromatization reactions, and improved accessibility to the acid sites can significantly increase the yielding of aromatics.[18] However, catalyst suffers from exceedingly fast deactivation by coking.[19] Some strategies have been proved to extend the life time of catalyst: (1) by the introduction of additional mesopores or reducing the crystal size, the diffusion path in zeolite can be reduced;[20–22] (2) grow catalyst in fluoride medium to minimize the framework defects;[23] (3) disperse zeolite by adding diluent for improve the heat transportation;[24] and (4) co-feeding some molecules to increase the combined H/C ratio of the bio-oil.[25]

This study sets out to elucidate the factors influencing the properties of the end-fuel, starting from organosolv lignin extraction from both hard- and softwood raw materials. The primary lignins are characterized in detail (^{13}C NMR and ^{1}H–^{13}C HSQC spectroscopy) and initially upgraded by hydrothermal liquefaction, with the characteristics of the obtained bio-oil fractions described (GC-MS and Fourier-transform ion cyclotron resonance mass spectrometry), before final catalytic upgrading is performed employing defect-free ultra-thin (35 nm) ZSM-5 catalyst. The catalyst was synthesized in fluoride medium and dispersed in 500 nm Stöber sol SiO_2, as these can significantly increase the diffusion of hydrocarbons and the transportation of heat generated by the exothermic reaction, respectively. In addition, the bio-oil upon conversion compositionally renders them closer to petroleum. As such, the current work provides a novel start-to-end investigation of lignocellulosic valorization with in-depth characterization of the various intermediate stages evaluated in light of the native material structure.

Materials and methods

Lignin isolation

Birch (B) and spruce (S) lignins were obtained through organosolv (conditions given in Table 1) as previously described.[26] In short, spruce and birch sawdust were treated at a solid-to-liquid ratio of 1-to-10 (dry weight biomass/volume solvent) in the presence or without acid catalyst (1% w/$w_{biomass}$). The solvent was a mixture of ethanol in water at a content of 60% v/v and 50% v/v for birch[26] and spruce sawdust, respectively. Subsequent the organosolv treatment, the slurry was vacuum-filtered to separate the solids from the liquid fraction. Lignin solubility was then reduced by removing/evaporating the ethanol by rotary evaporation allowing its isolation as precipitate. Subsequently, the precipitate was isolated by centrifugation (14 000 rpm/29 416 g, at 4 °C for 15 min) and then freeze-dried to yield the final powdery product.

Hydrothermal liquefaction (HTL)

An illustration of the set-up applied for the HTL is presented in Fig. 1. In short, it is a combination of three connected vessels. For trials performed in a semi-continuous fashion, the first reactor (semi-continuous feeding reactor in Fig. 1) is used as a feed tank where the starting feed is being stirred at room temperature. Next, when the feed liquid is pressurized, in this work by nitrogen at 55 bar, the feed is pushed into the pre-heated reactor (hydrothermal reactor in Fig. 1) by opening the valve for 0.5 seconds. All the valves in the hydrothermal system are pneumatic with on-off sensors to ensure safe operations. Initially, the pre-heated reactor contains 35 mL distilled water to ensure proper controller and thermometer function. When the desired treatment time is reached, the mixture is shot into a water-cooled cooling vessel (water-cooled vessel in Fig. 1)

Table 1 Conditions applied for organosolv fractionation of the respective lignocellulosic raw materials. For all treatments, the solid-to-liquid ratio applied was 1 gram biomass per 10 mL solvent

Code	Raw material	Temperature [°C]	Time [min]	EtOH [vol%]	Catalyst [H_2SO_4% w/$w_{biomass}$]
B	Birch sawdust	200	15	60	0.0
BA	Birch sawdust	200	15	60	1.0
S	Spruce sawdust	200	30	50	0.0
SA	Spruce sawdust	200	30	50	1.0

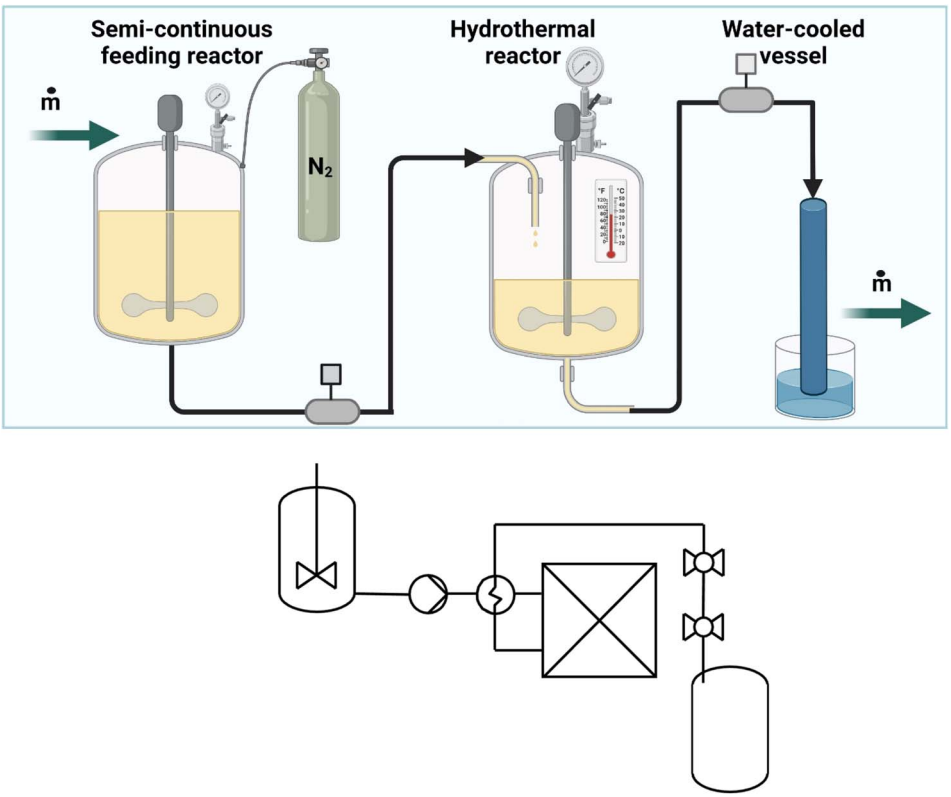

Fig. 1 Top: The experimental set-up used for HTL of lignin with ball valves separating the pressurized zones. Bottom: PI&D of the continuous HTL including feeding tank, pump, heat exchanger, reactor and pressure release valves.

using the remaining steam and nitrogen pressure in the reactor. Heating from room temperature to 320 °C is achieved within 20 min, while cooling back to room temperature is done within 5 min. In the semi-continuous system, initial trials used a 10% suspension of lignin in water (B, BA, S, SA).

The continuous reactor consists of a 5 L tank where the feed is stirred and pre-heated to 70 °C. Then with a dual-pumping system, the feed is fed into the reactor at 200 bar. Part of the feed stream is heated through a heat-exchanger system exchanging heat with the product stream, the remaining energy is obtained electrically until the desired temperature is obtained (PID controlled). At the end of the reaction time, the product is cooled down to 70 °C before being released through an alternating ball-valve system ensuring a pulse-flow operation. Overall reactor volume is 800 mL, and a flow-rate of 40 mL min^{-1} was applied. The residence time for the continuous system was 20 min. In the continuous system a 8.5% suspension of lignin in water was used.

The aqueous suspension in the crude reaction mixture was filtered over a 20 μm filter paper (Whatman 541). The filtrate was extracted twice with 50% of its volume of ethyl acetate to isolate the monomer rich light oil (LO). The remaining water phase was discarded. The HO and char were separated by washing the filter cake with 2-methyl-tetrahydrofuran (2-MeTHF). By removing the solvent, the HO is isolated. This fraction is the largest portion (see Fig. 3B) and is assumed to be comprised of depolymerized and deoxygenated species together with solvent-soluble unreacted lignin. An overview of the processing is presented in Fig. 2.

Quantitative ^{13}C nuclear magnetic resonance spectroscopy of the organosolv lignin

The lignin NMR analysis was performed as described previously.[27,28] In short, for quantitative ^{13}C NMR analysis, approx. 80 mg of lignin was dissolved in 500 μL DMSO-d_6. We applied 50 μL (~1.5 mg mL^{-1}) of Cr(III) acetylacetonate in DMSO-d_6 as a spin-relaxation agent and 50 μL (~15 mg mL^{-1}) of trioxane (92.92 ppm) in DMSO-d_6 as an internal standard. Spectra were recorded on a Bruker 600 MHz AVANCE III spectrometer equipped with a 5 mm BBO broadband ($^{1}H/^{19}F/^{2}D$) z-gradient cryo-probe and controlled with TopSpin 3.6.4 software at 30 °C, with a total of 20 000–24 000 scans. An inverse-gated proton decoupling pulse sequence was applied with a 90° pulse width, acquisition time of 1.2 s, and relaxation delay of 1.7 s. Data were processed with MestreNova Version 9.0.1 (Mestrelab Research S.L., Santiago de Campostela, Spain).

$^{1}H–^{13}C$ heteronuclear single quantum coherence (HSQC) analysis of the organosolv lignins

The same sample prepared for the acquisition of the quantitative ^{13}C NMR was used. HSQC spectra were obtained at 30 °C on a Bruker 600 MHz Avance III spectrometer (Bruker Biospin) controlled with Topspin 3.6.4 and equipped with a 5 mm BBO

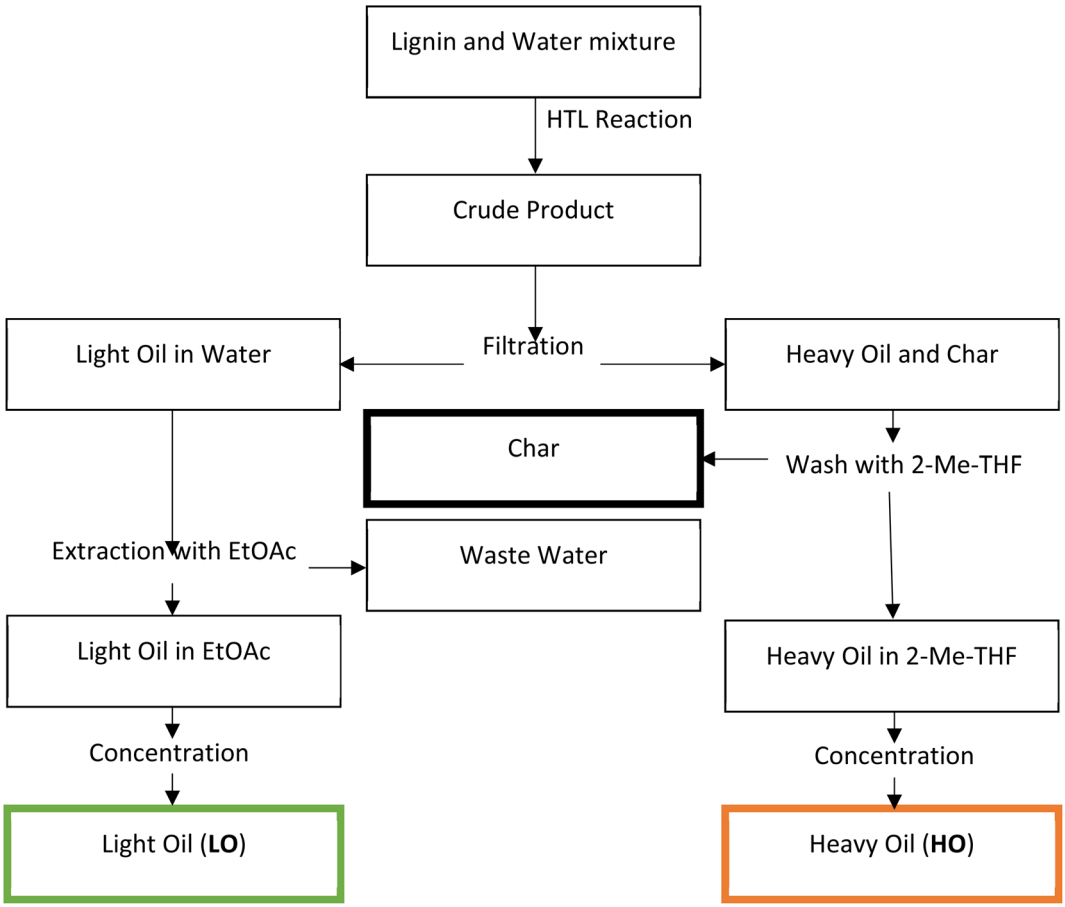

Fig. 2 An overall illustration of the workflow related to the HTL of lignin.

broadband ($^{1}H/^{19}F/^{2}D$) *z*-gradient cryo-probe. The Bruker hsqcetgpsisp2.2 pulse program in DQD acquisition mode was applied, with NS = 64; TD = 2048 (F2) and 512 (F1); SQ = 12.9869 ppm (F2) and 164.9996 ppm (F1); O2 (F2) = 2601.36 Hz and O1 (F1) = 7799.05 Hz; D1 = 2 s; CNST2 $^{1}J(C–H) = 145$; and acquisition time F2 channel = 197.0176 ms and F1 channel = 15.4164 ms. NMR data were processed with MestreNova.

GC/MS-analysis of light oil

The LO were analysed by GC-MS to determine the amounts of monomers. Therefore, the samples were dissolved in acetone. Guaiacol, 4-methylguaiacol (creosol), 3-methoxycatechol and 2,6-dimethoxyphenol (syringol) were used as standards for quantification.

Fourier-transform ion cyclotron resonance mass spectrometry (FT-ICR MS) of the heavy oil (HO)

The four heavy oils from liquefaction of birch or spruce lignin were prepared to a final concentration of 0.1 mg mL^{-1} in 90 : 10 (v/v) methanol/toluene (LC/MS grade).

Bio-oil mass spectra were acquired in positive-ion mode using atmospheric pressure photoionization (APPI) with a 7 T FT-ICR mass spectrometer (Solarix 2XR, Bruker Daltonics, Bremen, Germany). Ion source and instrument parameters were optimized *via* software FTMS-Control V2.3.0 (Bruker Daltonics). A 0.1 mg mL^{-1} sodium trifluoroacetate solution was used to externally calibrate the mass spectrometer, and to shim and gate the ICR detection cell. Mass spectra were acquired over a 193.5–2000 *m/z* range with a 4 megaword time-domain, and 300 scans were accumulated. Bio-oil samples were infused with a flow rate of 12 μL min^{-1}. The APPI source conditions were set with drying gas temperature and flow rate at 200 °C and 2 L min^{-1}, respectively, and the pressure of the nebulizer gas was 1.5 bar. The capillary voltage was 0.8 kV and the vaporizer was heated at 300 °C.

Software DataAnalysis 5.2 (Bruker, Daltonics) were used for data processing. Mass spectra were exported to peak list at a signal-to-noise ≥4. Internal calibration and peak list assignment were performed by Composer software (Sierra Analytics, Modesto, USA). Molecular formulae were assigned within a ±0.6 ppm mass error range, with the C, H, O, N, and S elements, and both radical cations and protonated ions were considered. This resulted to CH, CHO, CHN, CHON, and CHOS molecular series. The double bound equivalent (DBE) was calculated, as given by eqn (1), with n_C, n_H and n_N being number of carbon, hydrogen, and nitrogen atoms, respectively. The DBE *versus* carbon number (#C) graphs give information on the aromaticity and unsaturation degree of a molecule.

$$\mathrm{DBE} = 1 + n_C - \left(\frac{n_H}{2}\right) + \left(\frac{n_N}{2}\right) \quad (1)$$

Catalytic upgrading of the light oil fraction

The zeolite ZSM-5 catalyst used here comprised 35 nm thick defect free crystals synthesized in fluoride medium as described previously.[29] These defect free crystals are by far the thinnest reported, and it has been shown that these crystals displayed superior catalytic performance in terms of *e.g.* resistance to deactivation as compared with thicker ZSM-5 crystals and defective ZSM-5 crystals.[29] In the present work, these crystals were supported on spherical Stöber SiO_2 particles with a diameter of 500 nm in a ratio of 1 : 10. The mixture was pressed, crushed, and sieved to obtain a powder within the size range of 177 to 500 μm. Prior to use, the supported catalyst was dried at 110 °C for about 18 h.

For catalytic conversion of bio-oil, 1.7 g of the supported catalyst was loaded in a stainless-steel reactor with an inner diameter of 6 mm and a length of 140 mm. Quartz glass wool was used to keep the catalyst in the center of the reactor and graphite rings were used to seal the reactor. The bio-oil was mixed with methanol and water in a weight ratio of 60% bio-oil, 20% methanol, and 20% water or a ratio of 10% bio-oil, 30% methanol, and 60% water. A gas chromatograph (GC, Agilent 7890 B equipped with a capillary column CP-Sil PONA CB, 100 m × 250 μm × 0.5 μm and an FID detector) was connected online to the reactor.

The mixtures of bio-oil, methanol and water were fed at a weight hourly space velocity (WHSV) of 0.3 h^{-1} to the reactor at 360 °C, while the connection lines between the reactor and the GC were maintained at 220 °C. A stream of N_2 at a flow rate of 9.5 mL min^{-1} was used as carrier gas. The reactor effluent was sampled every 70 minutes by the GC. The observed GC-peaks could be classified into the following groups of products according to their retention times: deoxygenated C_5-products, *e.g.*, light alkenes and alkanes (all peaks except for methanol and for dimethyl ether (DME) were observed at retention time less than 9.8 min); deoxygenated C_{6+} products, *e.g.*, gasoline, (all peaks observed at retention time between 9.8 and 34 min); oxygenated products (all peaks observed with retention time greater than 34 min).

Results and discussion

Spruce sawdust

The lignins used in this work originate from spruce or birch sawdust, and while the specific mode of their extraction will affect their chemistry, they are also different from the start as they are isolated from soft- and hardwood, respectively.[11]

Considering the weight distributions from HTL of spruce lignins (S and SA; Fig. 3), employing acid (SA) during the lignin extraction process does not largely affect the LO yield, while that of HO increases. Inevitably, a certain amount of low molecular weight species are still liberated yielding a similar LO yield; however, less volatiles and water solubles, *i.e.*, substances lost with the waste water, are generated keeping more of the raw material in the HO fraction. To get an idea of the dynamics and what species are formed and potentially being either a precursor for either of the product fractions during the HTL, GC/MS-analysis was performed (Table 2).

Furthermore, in order to potentially unravel any correlation between generated LO monomers with the initial spruce lignins, qualitative ^1H–^{13}C HSQC and quantitative ^{13}C NMR analyses were performed on the two isolated spruce lignins. Quantization of the most common structures (Table 3) was achieved using the deviation of the HSQC data *via* quantitative ^{13}C NMR.

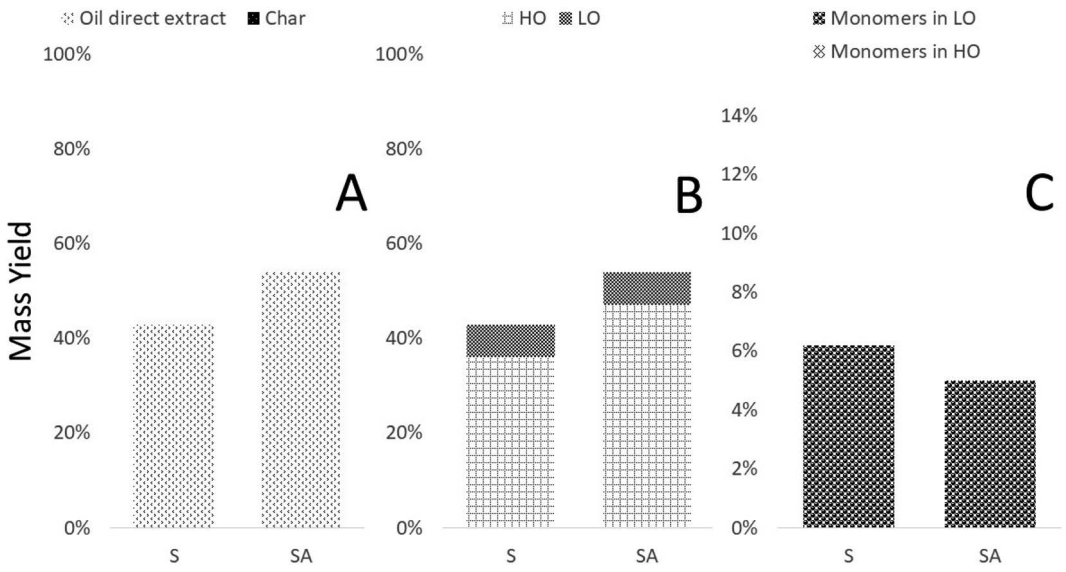

Fig. 3 Weight distributions of the various fractions originating from spruce-based lignins, either extracted with (SA) or without acid (S): (A) weight distribution of the non-volatile fractions obtained; (B) division of oil direct extract into HO and LO fractions; (C) distribution of monomers in the LO and HO fractions.

Table 2 Monomeric compounds and their relative content detected in the LO fraction of spruce (S and SA) and birch (B and BA) lignin samples

Compounds	S [mg monomers per g_{LO}]	SA [mg monomers per g_{LO}]	B [mg monomers per g_{LO}]	BA [mg monomers per g_{LO}]
p-Cresol	15.5	19.4		
Guaiacol	274.2	212.9	60.1	66.3
4-Methylguaiacol	113.3	73.7	24.1	45.1
3-Methoxycatechol	35.1		89.3	57.4
4-Ethylguaiachol	48.4	34.6	21.4	96.7
4-Methylcatechol		16		28.4
2,6-Dimethoxy phenol	62.5	17.4	251	215.9
4-Propylguaiacol	18.5	14.5	18	23.4
1,3,4-Dimethoxyphenol		16.7		20.2
Vanillin	76	56.9		40.5
5-Formylguaiacol			21.8	
Phenol, 2,6-dimethoxy-4-methyl	28.6		65.5	61.2
Acetoguaiacone	35.8	26.4	15.7	22.4
2,6-Di-*tert*-butyl-*p*-cresol			23.2	25.4
5-*tert*-Butylpyrogallol			33.5	
Guaiacylacetone	58.1	110.9	20.4	80.3
2-Butanone,4-(4-hydroxyphenyl)				30.4
Escaline				18.3
Syringaldehyde			23.3	
Gallacetophenone-4′-methylether				17.3
Benzenepropanol, 4-hydroxy-3-methoxy-	57.4	60.60		23
Syringaldehyde	19.1		39.8	52.2
Gallacetophenone-4′-methylether				17.1
Phenol (unknown)				24.4
Acetosyringone			28.7	56.2
Syringylacetone			42	121
5-(3-Hydroxypropyl)-2,3-dimethoxyphenol	26.2	18.2		
Phenol (unknown)		20.40		
Phenol (unknown)			18.1	
Phenol (unknown)	16.8	17.4		
Sum of quantified mass	885.5	716	796	1143
Monomers in fraction	89%	72%	80%	114%
Yield monomers in LO	6.2%	5.0%	5.6%	4.0%

The general distribution of motifs in lignins originating from relevant crops has been summarized[14] and will be applied as an initial foundation for the interpretation of the NMR data presented herein. In short, native lignins from softwoods are dominated by the guaiacyl monomer, derived from coniferyl alcohol. The interunit linkages vary, with the β-O-4′ linkage dominating (approx. 60%), while dibenzodioxocin (5–5′, 4-O-β′), phenylcoumaran (β-5′), and pinoresinol (β–β′) are usually present with contents of approx. 10, 10, and 5%, respectively. Apart from these more commonly occurring structures, spirodienone (β-1′) and biphenyl ether (4-O-5′) are present, albeit at significantly lower contents (approx. 1%). The analyses of the organosolv spruce lignins used for the HTL are in line with this general description, while indicating, however, that the standard motifs are drastically reduced in abundance. Analyses also indicate the presence of notable quantities of oxidized derivatives of typical interunit bonding motifs; condensation products are present.

The presented analytical data in form of GC-MS data and NMR data can serve to evaluate how the apparent structural changes in the raw-material, *i.e.*, lignin modification, including cross-coupling both in the aliphatic but also in the aromatic domains, potentially incorporating sugar dehydration products in form of lignin–humin–hybrid structures,[27] influences the dynamics and chemistry of the biomaterial during thermal treatment, thus determining final product formation.

Evaluating the results from Table 2, the monomers in the LO fraction with decreasing abundances as acid is used in the lignin extraction from spruce are guaiacol, 4-ethylguaiacol, and 4-methylguaiacol; this while the content of guaiacylacetone augments. The latter is understandable considering the data from the HSQC analysis in which G units with an oxidized side-chain are observed (Table 3). Importantly, liberated guaiacol units are in general decreasing abundancy in the LO fraction alongside a reduced overall monomer content, whereas the isolated HO fraction augments when moving from S to SA. For initially evaluating potential modification of the extracted lignins with respect to a putative lignin structure *in planta* during the initial organosolv process, the ^{13}C NMR spectra where used to generate rough estimates for the content of distinct aromatic carbons and to compare against the methoxyl group content (Table 3). In general, the total content of aromatic carbon atoms is presenting a 6-to-1 ratio relative the methoxyl groups, which matches fairly well with what to expect for a spruce lignin. However, the ArC-H content appears low: for an 'intact' guaiacyl monomer one would expect ratios of CH :

Table 3 Structural motifs and groups of the initial organosolv spruce (S) and birch (B) lignins quantified through NMR

		Spruce samples[a]		Birch samples[b]	
Motif (mode)	Shifts $\delta(^1H)$ [ppm]/$\delta(^{13}C)$ [ppm]	S [mmol g^{-1}]	SA [mmol g^{-1}]	B [mmol g^{-1}]	BA [mmol g^{-1}]
ArC-H	125.5–100.0	14.65	16.06	10.87	22.19
ArC-C	125.5–140.0	7.15	7.72	10.87	10.55
ArC-O-R	140.0–160.0	13.26	14.73	12.73	13.08
Ar(CH : CC : CO)		42 : 20 : 38	42 : 20 : 38	32 : 32 : 37	48 : 23 : 29
^{13}C–OMe (HSQC)	54.5–56.5	6.28 (5.55)	7.35 (6.59)	11.30 (11.49)	9.73 (9.98)
Sum aromatic carbons (per –OMe)		35.05 (5.58)	38.51 (5.24)	34.47 (3.05)	45.82 (4.71)
Ketone	206.50–207.10	0.50	0.42	0.00	0.04
β-O-4′ to S	4.88/72.04	0.03	0.03	0.36	0.10
	4.13/85.91				
	3.41/59.44				
β-O-4′ to G	4.90/71.34	0.01	0.02	0.19	0.03
	4.21/84.59				
	3.23/59.92				
β–β′	4.67/84.98	0.01	0.01	0.06	0.01
	3.06/53.50				
	4.03/70.99				
β-5′	5.43/87.00	0.02	0.02	0.19	0.08
	3.48/52.99				
	3.66/62.79				
Xylopyranoside	4.29/101.59	0.00	0.00	0.03	0.01
	3.06/72.49				
	3.26/73.94				
	3.51/75.35				
	3.36/62.50				
Benzyl ether (LCC)	4.59/80.92	0.00	0.01	0.04	0.01
Guaiacyl (G_6)	6.25–7.20/117.0–122.75	2.21	2.59	0.78	1.90
Ox. G_2	7.40/110.48	0.53	0.77	0.14	0.44
Guaiacyl (G_2 + furan B C_3)	G_2: 6.80–7.13/108.0–113.5	3.80	3.68	0.87	3.02
	G_2 + F_3: 6.42–6.98/109.5–113.8				
Furan B C_4	7.36–7.68/121.5–125.0	1.40	1.31	0.06	1.22
Syringyl ($S_{2,6}$)	6.20–7.00/101.8–104.4	0.07	0.07	2.34	1.39
Furan A C_3	6.15–6.75/104.4–107.4	0.12	0.18	0.69	2.99[c]
Furan A C_4	6.90–7.45/105.2–108.2	0.11	0.18	0.65	1.58
Sum furan rings		1.50	1.48	0.70	2.80
Sum lignin rings		2.28	2.66	3.11	3.29

[a] 200 °C; 30 min; 50 vol% EtOH. [b] 200 °C; 15 min; 60 vol% EtOH. [c] Overlapping signals.

CC : CO being approx. 3 : 2 : 1, whereby the ratios found are approx. CH : CC : CO = 2 : 1 : 2. Worth to mention is that the exact distribution of ArC-C and ArC-O carbons might experience overlaps caused by other structural motifs generating peaks in their respective regions, however, the tertiary aromatic carbon content obtained from ^{13}C NMR was found to match closely that obtained when integrating the HSQC spectra in the same regions, suggesting that tertiary carbons are reduced due to a higher content of quaternary aromatic carbons either linked to another carbon or oxygen. This trend appears to increase further as acid is employed in the extraction process, reducing still the number of aromatic carbons per measured methoxyl group. Interestingly, whereas the ratios of the various aromatic carbon types remain stable for the extraction treatments in absence (spruce lignin S) or presence of sulfuric acid (spruce lignin SA), the overall quantity increases for the latter alongside the oil-direct extract and amount of heavy oil (HO). Furthermore, the amount of monomers in the LO fraction decreases, suggesting that in fact the quantity and distribution of aromatic linkages influence how the oil fractions are distributed. Considering the composition of the LO fractions as elucidated through GC-MS, the monomers are largely of lignin origin, despite the fact that NMR analysis suggests the presence of furan moieties in the extracted lignins at significant contents (Table 3).

In order to evaluate the assigned lignin monomer and furan ring signals, the regions evaluated through ^{13}C NMR where compared against the shifts assigned through HSQC (Fig. 4). A good agreement is found regarding the contents obtained through ^{13}C NMR and their assigned HSQC shifts, using the quantification of the HSQCs on the basis of the quantitative ^{13}C NMR as reported before. Interestingly, the fit especially improves for spruce derived lignins when assuming that the majority of the G units carries only two aromatic CH carbons, which would imply that the majority carries an aromatic substitution.

For the spruce HO fractions, the results obtained by FT-ICR MS evidence an increase in CH species that originate on behalf

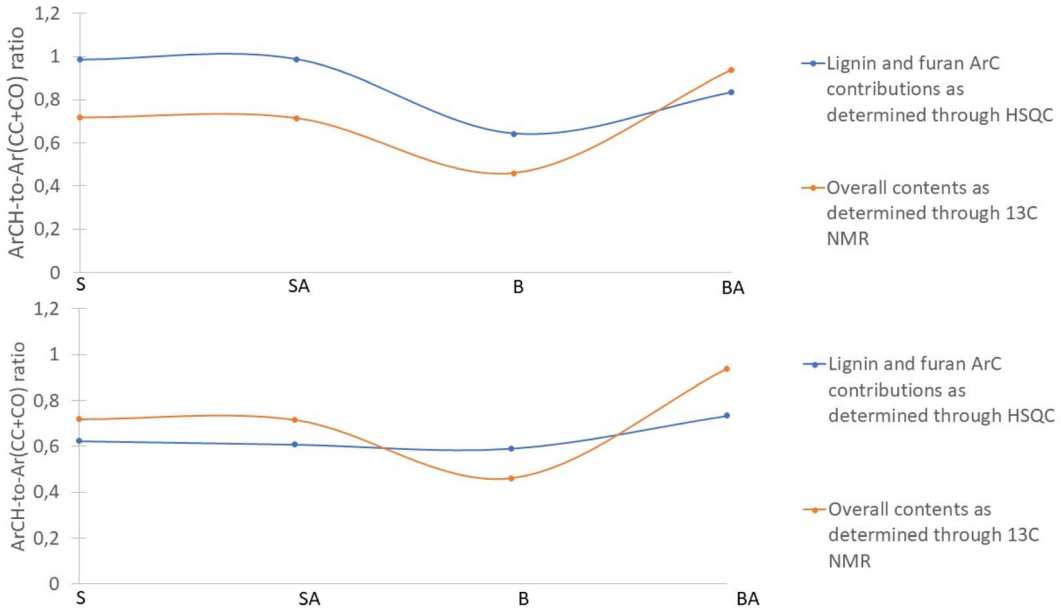

Fig. 4 Top: Ratio of tertiary to quaternary aromatic carbons as measured through ^{13}C shift ranges and specific $^{1}H–^{13}C$ assignments assuming that lignin monomers and furan rings are non-substituted. Bottom: As for the top figure except with the assumption that 1 of the 3 tertiary ring carbons of guaiacyl are substituted.

Table 4 Molecular composition description obtained by in APPI (+) FT-ICR MS of the HO fraction originating from spruce and birch lignins isolated in the absence (S, B) and presence (SA, BA) of acid-catalyst, with assignment number and corresponding percentages

Sample	CH	CHO	CHN	CHNO	CHOS	Total
S	251 (3.8%)	6240 (95.5%)	0	46 (0.7%)	0	6537
SA	810 (10.6%)	6597 (86.7%)	8 (0.1%)	127 (1.7%)	64 (0.8%)	7606
B	182 (2.5%)	6975 (95.2%)	5 (0.1%)	53 (0.7%)	112 (1.5%)	7327
BA	631 (8.2%)	6829 (89.2%)	0	50 (0.7%)	146 (1.9%)	7656

of CHO compounds (Table 4), in the sample obtained under acidic conditions, *i.e.*, SA. This does not contradict the NMR data where an increase in all aromatic carbon types (C–H, C–C, C–O) alongside the introduction of furans and aromatic substitution is observed. Fig. 5A also evidences the specificity of the spruce HO obtained under acidic conditions with the higher contribution of the CH species. For the CHO compounds, in both S and SA samples, the distribution is similar, although one can notice higher contribution of the oxygen-rich ($>O_9$) compounds in the SA sample (Fig. 5).

Similar observations are reported[30] and were attributed to repolymerization phenomena. Such oxygen-rich compounds can also represent larger molecular weight lignin-components obtained, or formed, by acid catalysis. Regarding the pure hydrocarbon species, an insight was achieved by representing them according to their DBE *vs.* carbon number (Fig. 6). The differences between S and SA samples are noticeable with more CH compounds in the SA sample. These specific features are characterized by components that are of higher molecular weight and that display a higher number of unsaturated motifs (higher DBE) components. It is also noteworthy that from species with C > 30 and DBE > 8, there are some packets that differ by 5–6 carbon atoms and 1–3 DBE units. These CH compounds specifically observed in the SA sample can originate from high-molecular weight lignin species that underwent deoxygenation reactions under acidic conditions. These high-molecular weight compounds can be imagined to be similar to those observed in Fig. S2,† in the form of CHO compounds from non-acid catalyzed organosolv lignin comprising close to 60 carbon atoms. Similar graphic analyses were done using CHO compounds (Fig. S2†), which did not evidence particular influence of acid addition during organosolv fractionation on the distribution of these species, unlike in case of the CH species. These results are in line with the distributions shown in Fig. 5A. Thus, these compounds detected by FT-ICR MS derive from lignin oligomers and comprise between 10 and 70 carbon atoms, which explains O-distributions with up to 16 oxygen atoms.[31] Relevant work performed which further aid the interpretation of the DBE *vs.* #C data suggest that, as acid is employed during the initial extraction treatment, the amount of saturated components augments within the produced HO fraction which potentially could be aliphatic segments linking aromatics.[32]

At this point it is also worth mentioning the appearance of 1,3,4-dimethoxyphenol in the LO derived from SA, hence the

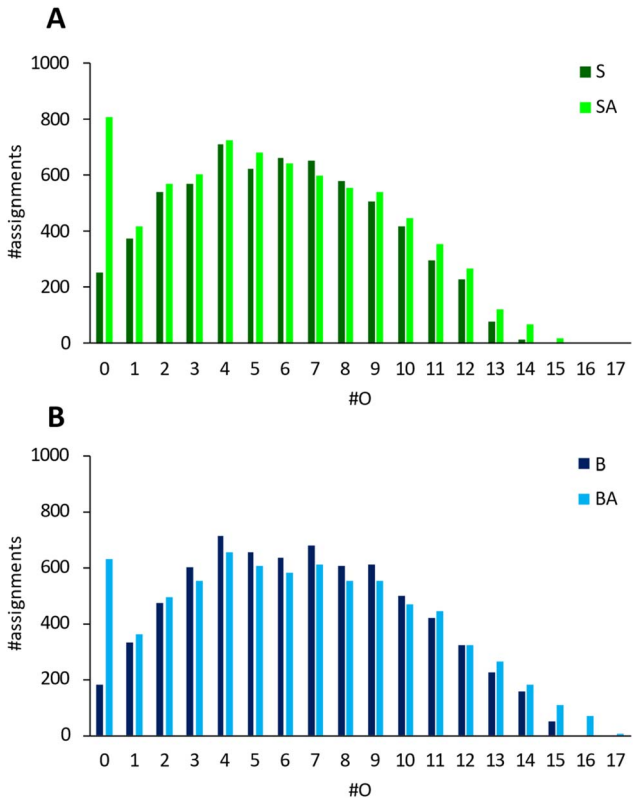

Fig. 5 Oxygen-distribution of CH and CHO compounds detected in HO of (A) spruce organosolv lignins extracted with (SA) or without acid (S) and (B) birch organosolv lignins extracted with (BA) or without (B) acid.

acid extracted spruce lignin (Table 1). This component was not detected in the S-derived LO fraction. Other double methoxylated species appeared in the spruce-derived LO fractions and are in contrast to what one would initially expect to in fractions generated from softwoods. It seems also important to point out that the HO fractions of spruce, most noteworthy as well as the HO fractions from birch (*vide infra*) show different characteristics (DBE *vs.* #C) compared to that of polyaromatic hydrocarbons (PAHs).[32,33] Instead, the DBE *vs.* #C slope suggest that aromatic groups carry increased contents of saturated carbon segments after HTL when acid is employed during the initial extraction.[32] Liberation of such segments during HTL could certainly justify the appearance of pure CH components.

Birch sawdust

Moving from spruce to the birch extracts, Fig. 7 illustrates that use of acid during the lignin isolation prevents subsequent char formation, but also reduces the LO yield while instead increasing the formation of HO.

Considering the lignin motifs elucidated through NMR (Table 3), there is a significant difference between their contents depending on whether one employs acid or not. For example, the β-O-4′ linkage content to either G or S units decreases from 0.19 and 0.36 to 0.10 and 0.03 mmol g^{-1}. Despite this, the overall changes in oil direct extract, char, HO and LO yield, are low compared to the spruce-derived products. When considering the distribution of aromatic carbons there is a large difference between B and BA. Especially the ArC-H content increases and is observed alongside a steep increase in the furan ring content (Table 2), which causes the sum of aromatic carbons per methoxyl to increase from the reasonable value of 3.05 to 4.71. This is not necessarily due to the introduction of furans considering that birch carries both guaiacyl and syringyl units and a value between 3 and 6 would be expected. Considering any aromatic substitutions (Fig. 4), the best fit for the aromatic carbon distributions, is found when not

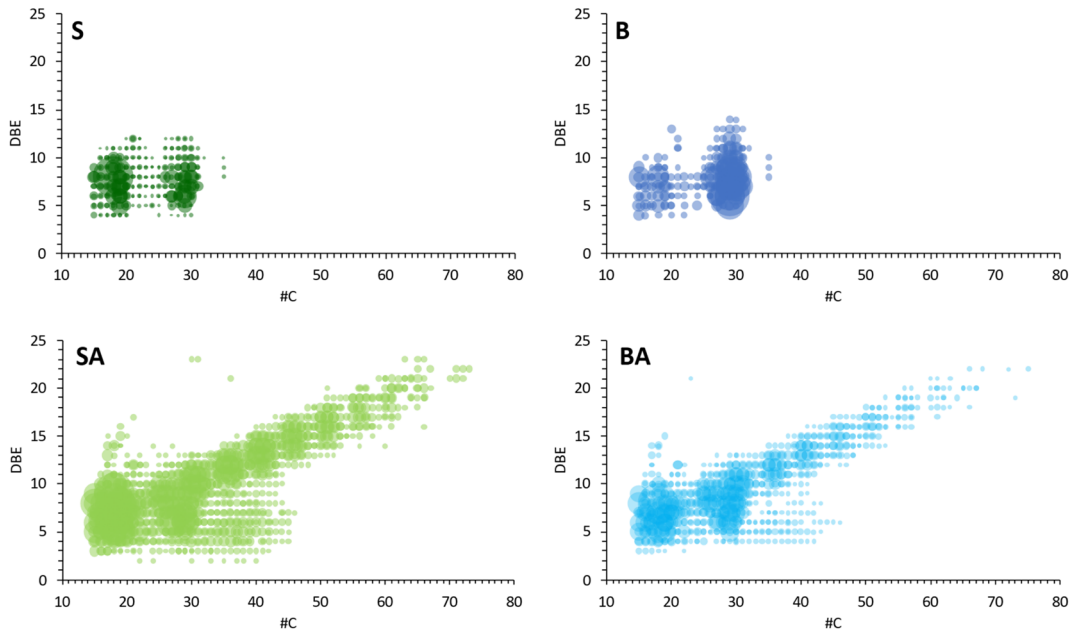

Fig. 6 DBE *vs.* carbon number graph of CH compounds detected by APPI FT-ICR MS of the four different HO obtained from spruce and birch lignins isolated in the absence (S, B) and presence (SA, BA) of acid-catalyst.

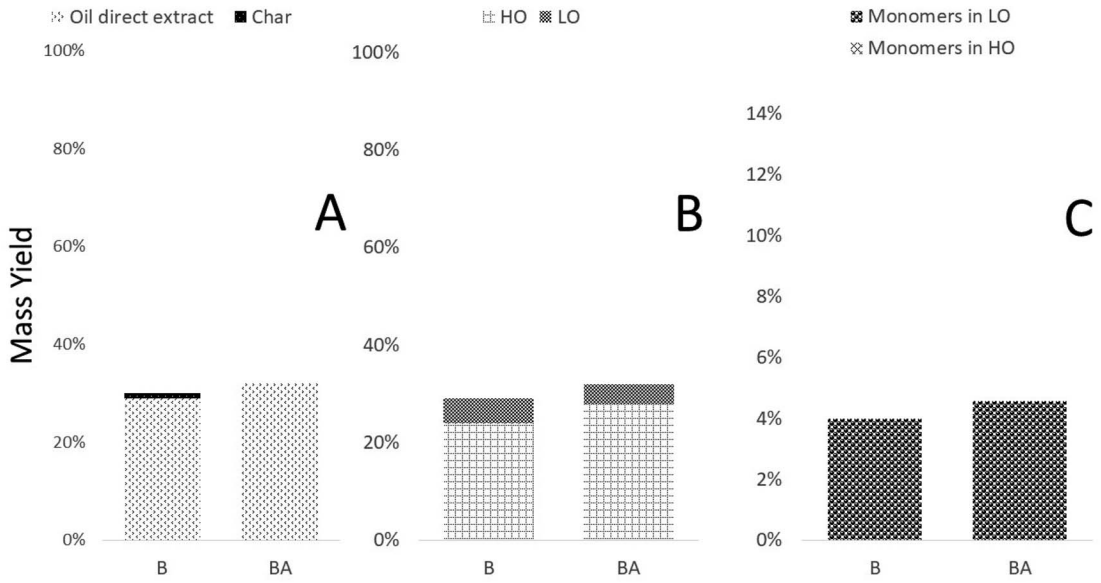

Fig. 7 Weight distributions of various fractions originating from birch-based lignins, either extracted with (BA) or without acid (B): (A) weight distribution of the non-volatile fractions obtained; (B) division of oil direct extract into HO and LO fractions; (C) distribution of monomers in the LO and HO fractions.

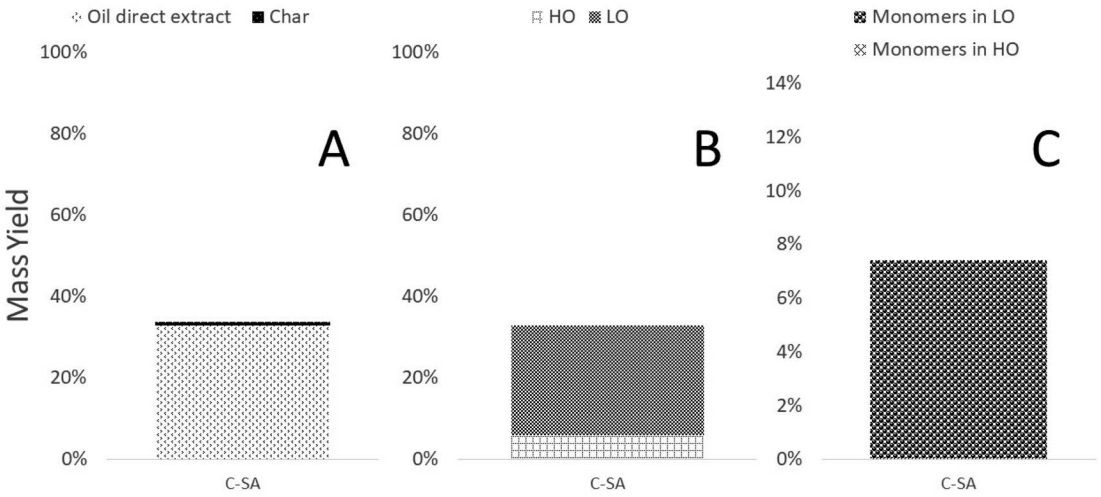

Fig. 8 Weight distributions of various fractions originating from spruce when process configuration was altered to continuous (C-SA): (A) weight distribution of the non-volatile fractions obtained; (B) division of oil direct extract into HO and LO fractions; (C) distribution of monomers in the LO and HO fractions.

assuming the presence aromatic condensation of the G unit and in general correlate well with the measured contents of lignin monomers and furans. Compared to the S and SA-derived bio-oils, the direct oil extract is far lower than for the birch, further indicating that aromatic cross-linking could promote retention in the HO fraction.

Moving to the GC-MS-analyses of the LO fraction (Table 2), there is an increase in the guaiacol compounds, which would seem reasonable when recollecting the reduction of β-O-4′ to G linkages. This is in contrast to what was observed for the spruce lignin where they instead decreased. Expected to be exclusive for the hardwood derived bio-oil, also syringyl derivates, *i.e.*, acetosyringone, syringylacetone, syringaldehyde, increase in content in LO when moving from B to BA and the same argument can be made from their β-O-4′ to S content. The differences between the BA fractions from softwood and the hardwood are also apparent looking at the total yields of monomers, even when considering an estimated error of 10% caused by the applied analyses, which is eventually biased by the fact that not all generated monomers are equally well ionizable: the total yields have been determined on the basis of the integrated area of the total ion chromatogram as obtained in the GC-MS analysis, causing in case of BA also a yield higher than 100%.

Table 5 Monomeric compounds and their relative content detected in the LO fraction of C-SA

Compounds	C-SA [mg monomers per g_{LO}]
Guaiacol	106
Catechol	19
Creosol	21
3-Methoxycatechol	3
4-Ethylguaiachol	17
5-Formylguaiacol	42
Acetoguaiacone	10
5-*tert*-Butylpyrogallol	41
Escaline	11
Syringaldehyde	2
Sum of quantified mass	272
Monomers in fraction	27%

As with the spruce-derived HO fractions, the ones from birch show a comparable behavior when considering the molecular distribution obtained from FT-ICR of the two HO fractions (Table 4 and Fig. 5B). There is also a significant increase of the pure hydrocarbons contribution when lignin is extracted with acid catalyst, however, less CH formulae were observed for BA compared to the SA sample. Also, whereas less developed than SA at higher carbon numbers, the same is indicated in Fig. 6 where the DBE *vs.* carbon number graph obtained from the CH assignments of the BA sample also display signal for compounds with C > 30 and DBE > 8. As for samples based on spruce-lignin, CHO compounds did not seem to be impacted by addition of acid during organosolv as shown by Fig. 5B and S2.†

Process modification

Continuous HTL. Moving towards an industrial feasible process, performing the HTL continuously would be of great advantage considering efficiency of production. For this purpose, spruce lignin (SA) was used and tested in a continuous HTL reactor. By switching from semi-continuous to continuous, heating time reduced from approx. 30 to 1–2 min (Fig. S1†) thus reducing thermal severity.

Considering the resulting weight distributions (Fig. 8), the most obvious change introduced by making the process continuous is that the majority of the biooil product is found to be LO. Also, for the first time in the present work, spruce lignin is found to generate char, albeit to a negligible amount. Previous findings have found that the LO yield increases on behalf of HO upon elevated HTL severity,[34] this while especially catechols have been found to be a precursor for bio-chars and active during repolymerization.[35] A striking difference between SA and C-SA is the differences in guaiacol and catechol contents in the LO where the former is reduced by more than 50% per gram LO, whereas catechol and creosol appear for the first time in this work (Table 5), suggesting that the LO from C-SA is to a larger degree developed. Guaiacol is considered the precursor of catechol,[36] with the latter tending to repolymerize into insoluble bio-char which makes the presented data reasonable. However, due to the lower thermal severity resulting from a more efficient heating, such a scenario must originate from the higher lignin loading applied during the continuous process.

Catalytic conversion of the light fraction of HTL oil. In a final trial, the LO fraction from BA was applied as feed for the catalytic conversion into short-chained, deoxygenated compounds. Fig. 9A illustrates the conversion and yields for the various group products for a feed consisting of 60% bio-oil BA-LO, 20% methanol, and 20% water. During the first 3.5 hours, a conversion higher than 97% is observed. However, after about 3.5 h, lower conversions are observed, presumably due to deactivation of the catalyst by coke formation.[29] It should be noted that if pure methanol is fed to the same catalyst at a very high WHSV of 8 h^{-1}, deactivation is observed after about 66 h, which would correspond to 1760 h (=66 h × 8/0.3) at a WHSV of 0.3 as in the present work. Initially, the yield (in mol) of deoxygenated C_{6+} molecules, *e.g.* gasoline, is as high as 50%, then it gradually reduced to almost 0% after 6 h. However, the yield of deoxygenated C_5-products is initially of 30%, and increased to about

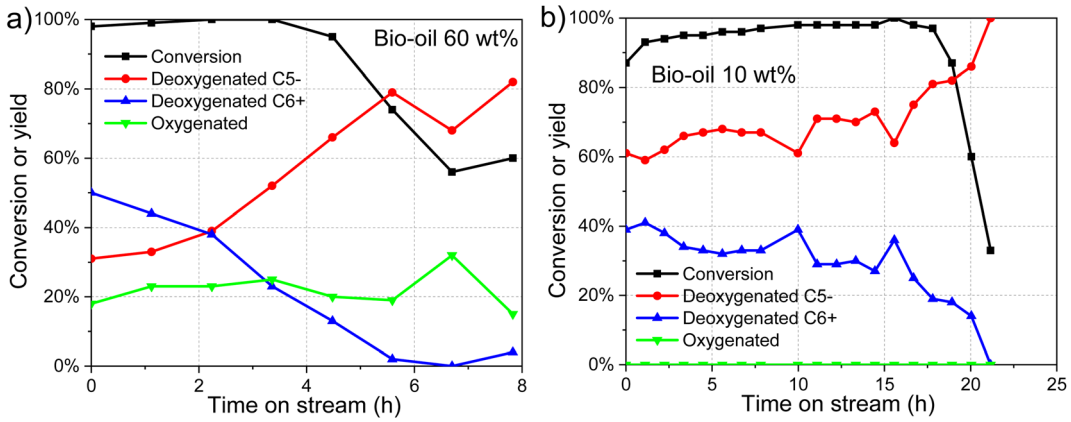

Fig. 9 Conversion of biooil and deoxygenated C_5- and deoxygenated C_{6+} yields (expressed as the percentage of the deoxygenated C_5- and deoxygenated C_{6+} in the final product) for different feeds for the catalytic conversion of the light fraction of HTL oil, as a function of time on stream at 360 °C and a WHSV of 0.3 h^{-1} over the 35 nm thick defect free ZSM-5 catalyst supported on 500 nm Stöber SiO_2 particles: (a) 60% bio-oil BA-LO, 20% methanol, and 20% water; (b) 10% bio-oil BA-LO, 30% methanol, and 60% water.

80% after about 6 h. The yield of oxygenated products remained unchanged at around 20%, and consequently the yield of deoxygenated products (*i.e.*, the sum of deoxygenated C_5- and deoxygenated C_{6+}), remained constant at about 80%. Fig. 9B illustrates the conversion and yields for a more dilute feed of the same bio-oil, *i.e.*, 10% bio-oil BA-LO, 30% methanol, and 60% water. In this case, the conversion was higher than 90% for about 18 h before the catalyst deactivated. Consequently, when the bio-oil is six times more dilute, deactivation is observed five times later, *i.e.*, the time to deactivation is nearly proportional to the flowrate of bio-oil. Similar trends were observed for the yields of C_5-products (increasing with time) and the yield of C_{6+} products (decreasing with time). The yield of the oxygenated product remained at close to 0% during the entire experiment.

Conclusion

Lignins extracted through organosolv processing, from spruce or birch, with or without sulfuric acid as acidic catalyst display varying chemical structures, which dictate how they behave upon formation of bio-oil during hydrothermal liquefaction. For spruce lignins, its innate 'sensitive' nature toward depolymerization and cross-coupling generate a bio-oil precursor, which upon HTL has the potential of generating an enlarged fraction of heavy oil (HO). The birch lignin experiences overall less modification, and despite similarities in terms of trends observed upon acid-catalyzed lignin extraction from birch when compared to spruce, the more 'resistant' nature of the hardwood lignin creates a starting-point where depolymerized traditional motifs refrain from undergoing further structural modifications that would give raise to an enhanced formation of the HO fraction as observed for the spruce-derived lignins. In addition, continuous processing was evaluated and found to primarily generate LO when SA was evaluated, *i.e.*, a softwood lignin isolated using an acid-catalysed organosolv process. Finally, the LO fraction obtained from BA, *i.e.*, lignin extracted using the acid-catalysed organosolv process, was catalytically converted to short-chained deoxygenated compounds with a conversion yield of more than 97%, prior to catalyst deactivation after approx. 18 h.

Author contributions

PPT: investigation, data analysis, writing – original draft; JF: investigation, data analysis, writing – review & editing; HL: data analysis, supervision, writing – original draft; JH: investigation, data analysis, writing – review & editing; VC: investigation, data analysis, writing – review & editing; MZ: investigation, data analysis; AT: data analysis, writing – review & editing; FA: data analysis, supervision, writing – review & editing; JH: data analysis, methodology, supervision; TG: conceptualization, methodology, data analysis, supervision, writing – review & editing; UR: conceptualization, methodology, supervision, writing – review & editing; PC: conceptualization, methodology, supervision, writing – review & editing; LM: conceptualization, methodology, data analysis, supervision, writing – original draft.

Conflicts of interest

There are no conflicts to declare.

Acknowledgements

This work was part of the projects "Upgrading of organosolv lignin to jet fuel (GOLdJET FUEL)" and "Eco-efficient biorefinery for competitive production of green renewable shipping fuels (ECO-FORCE FUELS)" funded by the Swedish Energy Agency with reference numbers 2019-005832 and 2022-201046 respectively. Mattias Hedenström, Swedish NMR Centre (Umeå, Umeå University, VR RFI), João Figueira, Swedish NMR Centre (Umeå, Umeå University, Scilife Lab) and the NMR Core Facility (Swedish NMR Centre, SwedNMR, Umeå node), Umeå University are acknowledged for NMR support. FTICR MS equipment was funded by the European Regional Development Fund (FEDER), the general council of Moselle, Region Grand Est, Metz Metropole and the University of Lorraine (RESEX project).

References

1 I. v. Provornaya, I. v. Filimonova, V. Y. Nemov, A. v. Komarova and Y. A. Dzyuba, *Energy Rep.*, 2020, **6**, 514–522.
2 U. Bardi, *Energy Res. Soc. Sci.*, 2019, **48**, 257–261.
3 *Climate Change 2022: Impacts, Adaptation and Vulnerability|Climate Change 2022: Impacts, Adaptation and Vulnerability*, **https://www.ipcc.ch/report/ar6/wg2/**, accessed 10 May 2022.
4 J. Podesta and P. Ogden, *Wash. Q.*, 2008, **31**, 115–138.
5 J. Gornall, R. Betts, E. Burke, R. Clark, J. Camp, K. Willett and A. Wiltshire, *Philos. Trans. R. Soc., B*, 2010, **365**, 2973–2989.
6 L. Dessbesell, M. Paleologou, M. Leitch, R. Pulkki and C. Xu, *Renewable Sustainable Energy Rev.*, 2020, **123**, 109768.
7 J. Zakzeski, P. C. A. Bruijnincx, A. L. Jongerius and B. M. Weckhuysen, *Chem. Rev.*, 2010, **110**, 3552–3599.
8 P. C. A. Bruijnincx and B. M. Weckhuysen, *Nat. Chem.*, 2014, **6**, 1035–1036.
9 D. Wei Kit Chin, S. Lim, Y. L. Pang and M. K. Lam, *Biofuels, Bioprod. Biorefin.*, 2020, **14**, 808–829.
10 P. P. Thoresen, L. Matsakas, U. Rova and P. Christakopoulos, *Bioresour. Technol.*, 2020, **306**, 123189.
11 C. Sun, G. Song, Z. Pan, M. Tu, M. Kharaziha, X. Zhang, P.-L. Show and F. Sun, *Bioresour. Technol.*, 2023, **368**, 128356.
12 W. J. J. Huijgen, A. T. Smit, J. H. Reith and H. den Uil, *J. Chem. Technol. Biotechnol.*, 2011, **86**, 1428–1438.
13 F. Hu, S. Jung and A. Ragauskas, *Bioresour. Technol.*, 2012, **117**, 7–12.
14 J. Ralph, C. Lapierre and W. Boerjan, *Curr. Opin. Biotechnol.*, 2019, **56**, 240–249.
15 A. R. K. Gollakota, N. Kishore and S. Gu, *Renewable Sustainable Energy Rev.*, 2018, **81**, 1378–1392.
16 S. S. Toor, L. Rosendahl and A. Rudolf, *Energy*, 2011, **36**, 2328–2342.
17 A. N. Kay Lup, F. Abnisa, W. M. A. W. Daud and M. K. Aroua, *Appl. Catal., A*, 2017, **541**, 87–106.

18 A. J. Foster, J. Jae, Y.-T. Cheng, G. W. Huber and R. F. Lobo, *Appl. Catal., A*, 2012, **423–424**, 154–161.
19 P. A. Alaba, Y. M. Sani, I. Y. Mohammed and W. M. A. Wan Daud, *Rev. Chem. Eng.*, 2016, **32**(1), 71–91.
20 A. Veses, B. Puértolas, J. M. López, M. S. Callén, B. Solsona and T. García, *ACS Sustain. Chem. Eng.*, 2016, **4**, 1653–1660.
21 J. Hertzog, V. Carré, L. Jia, C. L. Mackay, L. Pinard, A. Dufour, O. Mašek and F. Aubriet, *ACS Sustain. Chem. Eng.*, 2018, **6**, 4717–4728.
22 L. Y. Jia, M. Raad, S. Hamieh, J. Toufaily, T. Hamieh, M. M. Bettahar, G. Mauviel, M. Tarrighi, L. Pinard and A. Dufour, *Green Chem.*, 2017, **19**, 5442–5459.
23 Z. Qin, L. Lakiss, L. Tosheva, J.-P. Gilson, A. Vicente, C. Fernandez and V. Valtchev, *Adv. Funct. Mater.*, 2014, **24**, 257–264.
24 I. Yarulina, F. Kapteijn and J. Gascon, *Catal. Sci. Technol.*, 2016, **6**, 5320–5325.
25 U. V. Mentzel and M. S. Holm, *Appl. Catal., A*, 2011, **396**, 59–67.
26 M. Monção, K. Hrůzová, U. Rova, L. Matsakas and P. Christakopoulos, *Molecules*, 2021, **26**, 6754.
27 P. P. Thoresen, H. Lange, U. Rova, P. Christakopoulos and L. Matsakas, *Int. J. Biol. Macromol.*, 2023, **233**, 123471.
28 P. P. Thoresen, H. Lange, C. Crestini, U. Rova, L. Matsakas and P. Christakopoulos, *ACS Omega*, 2021, **6**, 4374–4385.
29 J. Hedlund, M. Zhou, A. Faisal, O. G. W. Öhrman, V. Finelli, M. Signorile, V. Crocellà and M. Grahn, *J. Catal.*, 2022, **410**, 320–332.
30 P. D. Kouris, X. Huang, X. Ouyang, D. J. G. P. van Osch, G. J. W. Cremers, M. D. Boot and E. J. M. Hensen, *Catalysts*, 2021, **11**, 750.
31 E. Terrell, V. Carré, A. Dufour, F. Aubriet, Y. Le Brech and M. Garcia-Pérez, *ChemSusChem*, 2020, **13**, 4428–4445.
32 R. Luo and W. Schrader, *J. Hazard. Mater.*, 2021, **418**, 126352.
33 A. T. Juarez-Facio, C. Castilla, C. Corbière, H. Lavanant, C. Afonso, C. Morin, N. Merlet-Machour, L. Chevalier, J.-M. Vaugeois, J. Yon and C. Monteil, *J. Environ. Sci.*, 2022, **113**, 104–117.
34 E. Miliotti, S. Dell'Orco, G. Lotti, A. Rizzo, L. Rosi and D. Chiaramonti, *Energies*, 2019, **12**, 723.
35 S. Kang, X. Li, J. Fan and J. Chang, *Renewable Sustainable Energy Rev.*, 2013, **27**, 546–558.
36 J. Schuler, U. Hornung, N. Dahmen and J. Sauer, *GCB Bioenergy*, 2019, **11**, 218–229.